Polarization independent blue-phase liquid crystal cylindrical lens with a resistive film

Yan Li,[1] Yifan Liu,[1] Qing Li,[2] and Shin-Tson Wu[1,*]

[1]CREOL, The College of Optics and Photonics, University of Central Florida, Orlando, Florida 32816, USA

[2]Display R&D Center, School of Electronic Science and Engineering, Southeast University, Nanjing 210096, China

*Corresponding author: swu@mail.ucf.edu

Received 26 January 2012; revised 28 February 2012; accepted 1 March 2012;
posted 1 March 2012 (Doc. ID 162187); published 7 May 2012

We propose a new electrode design for polarization-independent cylindrical lens using a polymer-stabilized blue phase liquid crystal (BPLC). The top electrode is coated with a transparent and resistive film to generate linearly varying electric potential from center to edge; while the bottom iridium tin oxide electrode has a constant potential. Therefore, the vertical electric field across the BPLC layer varies linearly over the lens aperture and a desired parabolic phase profile is obtained automatically according to the Kerr effect. Simulation results show that this simple device is polarization independent and it has parabolic-like phase profile in a large tuning range. © 2012 Optical Society of America

OCIS codes: 110.1080, 230.3720.

1. Introduction

The focal length of an adaptive liquid crystal (LC) lens [1–14] can be tuned continually by an external voltage without any mechanical moving part. Several methods have been developed to control the phase profile across the lens aperture. Among them, hole-patterned structure [8–10] with a dielectric layer on the inner surface of the substrate could generate a smooth phase profile, but the shielding from the dielectric layer increases the operating voltage noticeably. Multi-electrode structure [11,12] could generate the desired phase profile by individually addressing the pixelated electrodes, but the driving is complicated. Moreover, to have a smoother phase profile, more electrodes and closer spacing are needed. As a result, diffraction may become severe. Another method called modal LC lens [13,14], with a planar high resistant electrode, can realize a smooth phase profile without pixelated electrodes. Most adaptive lenses using nematic LCs are polarization dependent and have a relatively slow response time, especially when a thick LC layer is involved.

Recently, polymer-stabilized blue-phase liquid crystal (BPLC) [15–21] has found useful applications in photonic devices because of its submillisecond gray-level response time [22,23]. A hole-patterned [24] microlens using a polymer-stabilized BPLC was demonstrated experimentally with a fast response time and polarization insensitivity. The device structure is fairly simple, but the phase profile is not ideal and consequently, its image quality is compromised. Polarization independent blue-phase lens using a curved iridium tin oxide (ITO) electrode was proposed [25], but the fabrication of such structures seems complicated. Another BPLC gradient-index lens with planar multi-electrodes [26] was proposed to realize parabolic phase profile at different focal lengths by addressing the pixelated electrodes individually, but it requires a high dielectric constant layer to overcome the polarization effect.

In this paper, we propose a new cylindrical microlens using a polymer-stabilized BPLC. The BPLC is sandwiched between a planar resistive electrode and a planar ITO electrode. A parabolic phase profile is

1559-128X/12/142568-05$15.00/0

obtained in the low field region due to the linear Kerr effect in the BPLC layer with only one data addressing. Our design has a larger optical power compared to those shown in [25,26] at the same voltage, because there is no shielding effect from any dielectric layer. Simulation results show that this simple device is polarization independent and it has parabolic-like phase profile in a large tuning range.

2. Device Configuration and Working Principle

Figure 1 shows the side view of our proposed cylindrical BPLC lens. On the inner surface of top substrate, there is a center ITO electrode strip at the center of the lens, and two ITO electrode strips on the two edges, respectively. The aperture of the lens is further coated with a thin transparent high-resistive film. On the inner surface of the bottom substrate, a planar ITO electrode is coated. The radius of aperture is R, and the cell gap of BPLC layer is d_{LC}.

In our design, we ground the center ITO electrode ($x \approx 0$) and bottom ITO electrode, but vary the voltage (V_0) on the edge electrodes ($x \approx R$). When $V_0 = 0$, there is no electric field and the BPLC remains optically isotropic. For the normally incident light, both the optical waves (here wave 1 is defined as the wave polarized in y direction, and wave 2 polarized in x direction) experience n_{iso} at any radius. Thus, there is no optical power.

When $V_0 > 0$, we could obtain a differential equation for the potential distribution on the resistive film [27,28]:

$$\nabla^2 V = \frac{\rho_R \omega \varepsilon' j}{d_R d_{\mathrm{LC}}} V + \frac{\rho_R \omega \varepsilon''}{d_R d_{\mathrm{LC}}} V, \tag{1}$$

where ρ_R is the resistivity of the resistive film, d_R and d_{LC} are the thicknesses of the resistive film and LC, respectively, ω is the AC frequency, and ε' and ε'' are the real and imaginary parts of LC dielectric constants. Since the aperture dimension is much larger than the resistive film thickness, and it is a cylindrical lens, the electric field in x direction is much larger than those in other two directions within the resistive film. Combining the boundary condition $V|_{x=0} = 0$, Eq. (1) has an approximate solution:

$$V = a\left[\exp\left(\sqrt{c}\exp\left(\left(\frac{\pi}{4} - \frac{\theta}{2}\right)j\right)x\right) - \exp\left(-\sqrt{c}\exp\left(\left(\frac{\pi}{4} - \frac{\theta}{2}\right)j\right)x\right)\right], \tag{2}$$

where a is a positive real constant, $c = \frac{\rho_R \omega |\varepsilon^*|}{d_R d_{\mathrm{LC}}}$, $\varepsilon^* = \varepsilon' - \varepsilon'' j = |\varepsilon^*| \exp(-j\theta)$, and θ the phase delay between ε'' an ε'.

When $\sqrt{c}|x| \ll 1$, using Taylor expansion, the amplitude of potential distribution can be approximated as:

$$|V| \approx 2a\sqrt{c}|x|, \tag{3}$$

where $\rho_R = 0.01\ \Omega \cdot \mathrm{m}$ (a typical value of poly(3,4-ethylenedioxythiophene) resistive film), $\omega = 200\pi$ rad/s, $d_R \sim 30$ nm, $d_{\mathrm{LC}} \sim 10\ \mu$m, $\varepsilon' = 53\varepsilon_o$, $\varepsilon'' = 3.18\varepsilon_o$, $\varepsilon_o = 8.85 \times 10^{-12}$F/m, and $|x| \le R = 100\ \mu$m. Then, $\sqrt{c}|x| \le 0.0087 \ll 1$, and linear potential distribution condition is fulfilled, and the potential could be expressed as

$$|V| = \frac{|x|}{R} V_0. \tag{4}$$

As a result, vertical electric fields with gradient intensity are generated across the lens and so is induced birefringence Δn_{ind}. For a normally incident light, both waves 1 and 2 see an ordinary refractive index $n_0 = n_{\mathrm{iso}} - \Delta n_{\mathrm{ind}}/3$ [21], which is also radius dependent. Near the center of the lens, the electric fields are weaker due to smaller voltage difference between top and bottom electrodes; thus, the induced birefringence Δn_{ind} is smaller and n_o is larger. On the other hand, near the edge of the lens, the induced birefringence is larger and n_o is smaller. Therefore, a phase profile with positive lens is formed.

At the low field region, the induced birefringence follows the Kerr effect [29]:

$$\Delta n_{\mathrm{ind}} = \lambda K E^2, \tag{5}$$

where λ is the wavelength and K is the Kerr constant. At radius r, considering the linear potential distribution in Eq. (4), the induced birefringence could be further expressed as:

$$\Delta n_{\mathrm{ind}} = \lambda K E^2 = \lambda K \frac{V^2}{d_{\mathrm{LC}}^2} = \lambda K \frac{V_o^2}{d_{\mathrm{LC}}^2 R^2} x^2. \tag{6}$$

Equation (6) is a parabolic function with respect to location x. Consequently, the phase $\Phi(x) = 2\pi d_{\mathrm{LC}} n_o/\lambda = 2\pi d_{\mathrm{LC}}[(n_{\mathrm{iso}} - \Delta n_{\mathrm{ind}}/3)]/\lambda$ would also have a parabolic shape. With such a simple structure, we could obtain parabolic phase profile easily.

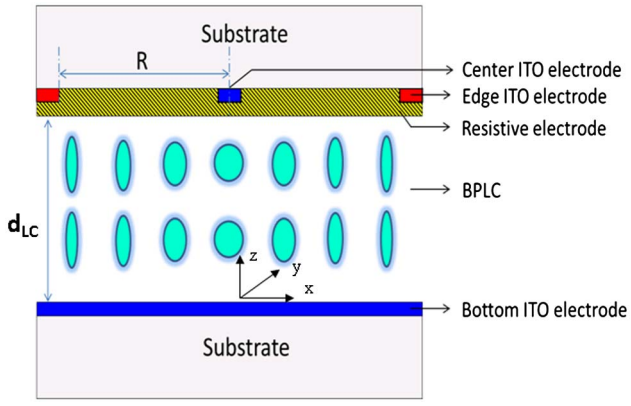

Fig. 1. (Color online) Side view of the proposed cylindrical BPLC lens.

However, as the electric field further increases, the induced birefringence would gradually saturate according to the extended Kerr effect [30]:

$$\Delta n_{\mathrm{ind}} = \Delta n_{\mathrm{s}}[1 - \exp(-(E/E_{\mathrm{s}})^2], \tag{7}$$

where Δn_s is saturation induced birefringence of the BPLC composite and E_s is the saturation electric field. Therefore, the phase profile would deviate from the ideal parabolic shape in the high field region.

3. Simulation Results

In order to validate the device concept, we carried out simulations using finite-difference frequency-domain method. We use the linear gradient potential on the resistive film as the boundary condition for BPLC cell. We first calculated the electric field distribution in the LC layer, then got the induced birefringence based on extended Kerr model as shown in Eq. (7) and finally the phase for the waves 1 and 2. The BPLC we used is Chisso JC-BP01M [31]. It has $E_s \approx 5.4$ V/μm and $\Delta n_s \approx 0.14$ at $\lambda = 633$ nm and used room temperature. For practical applications, we are more interested in $\lambda = 550$ nm. Thus, we extrapolated the Δn_s to $\lambda = 550$ nm based on the wavelength dispersion model [32] and found $\Delta n_s \approx 0.1487$. Since E_s does not depend on the wavelength, it remains the same.

Figure 2 shows the simulated phase profiles of the proposed lens structure with different cell gaps at $50V_{\mathrm{rms}}$ operating voltage and $\lambda = 550$ nm. The widths of center and edge electrodes are both 2 μm, and the aperture radius is 100 μm. The black solid curve and red dotted curve represent the phase profiles of wave 1 and wave 2, respectively, in a structure with $d = 8$ μm; and the pink solid curve and blue dotted curve represent the phase profiles of wave 1 and 2, respectively, in a structure with $d = 25$ μm. First of all, at the same applied voltage $50V_{\mathrm{rms}}$, the 8 μm structure has more than 1π phase difference from center to edge, while the 25 μm structure has only $\approx 0.6\pi$. Although the 25 μm LC layer would potentially have much larger phase difference at higher voltage, at this specific voltage, its phase is smaller due to the much weaker electric fields. Meanwhile, inside the 8 μm structure, electric fields are so strong that the induced birefringence deviates from the Kerr relation. As a result, the phase profile also deviates from the ideal parabolic shape. In the 25 μm lens cell, the deviation is much smaller so that phase profile is nearly parabolic. For our BPLC lens structure, there is a critical electric field instead of critical voltage, beyond which, the deviation from the Kerr effect is so much that the phase profile could not be regarded approximately as parabolic anymore. This critical field is determined by the liquid crystal material. Obviously, a larger cell-gap structure promises a better phase profile at the same voltage.

Second, the 8 μm structure has a better overlap between waves 1 and 2. The thinner the cell gap is, the stronger the vertical components of electric fields are, and, relatively, the smaller the horizontal components. As discussed in [25], horizontal electric field components are the causes of polarization dependency, since wave 1 would see a decreased refractive index, while wave 2 sees an increased one. With a relatively smaller horizontal component, smaller cell gap is more advantageous for polarization independency. Similarly, a larger aperture would result in a better overlap of the two waves.

So we have chosen an optimized structure with $d = 13$ μm and $R = 100$ μm, to have a large optical path length difference, good phase profile shape and polarization independency at the same time. As shown in Fig. 3, at $50V_{\mathrm{rms}}$ a phase change $\sim\pi$ is achieved. Wave 1 (black solid curve) and wave 2 (red dotted curve) overlap with each other very well, indicating the optimized structure is indeed polarization independent. Moreover, they fit with the ideal parabolic shape (blue dashed curve) well. Thus, a good image quality could be obtained. Obviously, the lower the operating voltage, the more parabolic-like shape it would form, as shown by the $30V_{\mathrm{rms}}$ curves, because the induced birefringence follows the Kerr effect better in the low field region.

Figure 4 shows electric field distribution across the BPLC lens where $|E_z|$ is much larger than $|E_x|$. That is why the device is polarization independent [25]. To further suppress the difference between the phase profiles of the two polarizations, one could add a dielectric layer beneath the resistive film to shield

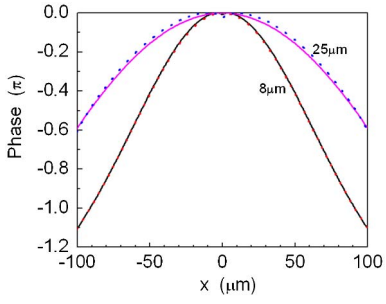

Fig. 2. (Color online) Simulated phase profiles ($\lambda = 550$ nm) across the lens for wave 1 (solid lines) and wave 2 (dotted curves) at $V_o = 50V_{\mathrm{rms}}$. The upper curve is for $d = 25$ μm lens and the lower one is for $d = 8$ μm.

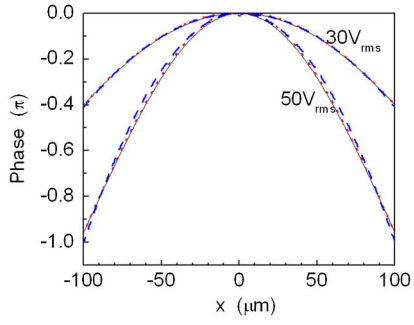

Fig. 3. (Color online) Simulated phase profiles ($\lambda = 550$ nm) across the lens with a 13 μm cell gap at $30V_{\mathrm{rms}}$ and $50V_{\mathrm{rms}}$. Black solid curves are for wave 1, red dotted curves are for wave 2, and blue dashed curves are ideal parabolic curves.

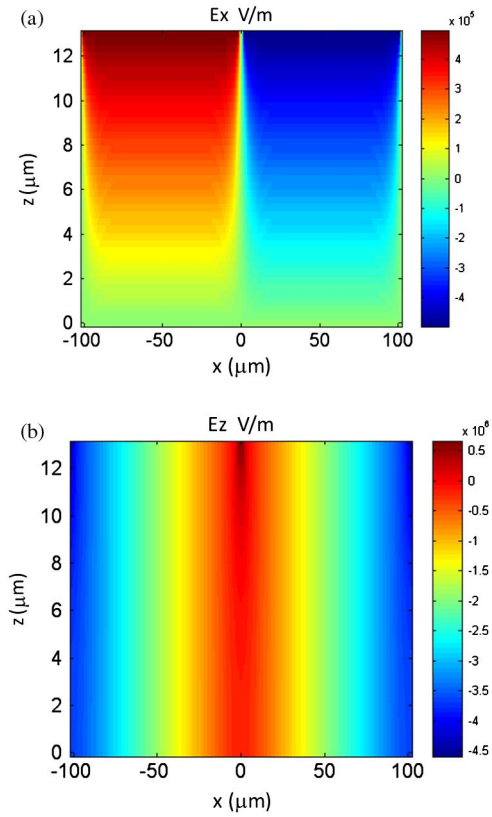

Fig. 4. (Color online) Electric field distribution across the BPLC cylindrical lens with 13 μm cell gap at $50V_{\mathrm{rms}}$, (a) for E_x and (b) for E_z.

those horizontal electric fields. From Fig. 4, we could see electric fields are below the saturation electric field E_s. Therefore, it follows the Kerr model very well, and consequently, the phase profile has a nice parabolic shape.

Figure 5 shows the simulated voltage dependent focal length for the abovementioned optimized structure. The focal length is calculated using the following equation [25,26]:

$$f = R^2/2\delta n(E)d_{\mathrm{LC}}, \tag{8}$$

where $\delta n(E)$ is the refractive index difference between the lens center and edge. The black solid curve is the focal length for wave 1, and the red dashed curve is for wave 2. As shown in Fig. 5, the two waves have the same focal length, which further proves the lens is polarization independent. As voltage increases, the focal length decreases. At $50V_{\mathrm{rms}}$, the simulated focal length is about 18 mm.

A possible extension of present lens structure is to have the edge electrode and bottom electrode grounded, while varying the voltage on the center electrode. Then a negative lens is formed, but the shape of the lens will not be as good as the positive lens.

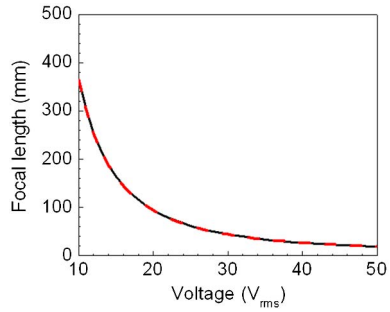

Fig. 5. (Color online) Simulated voltage dependent focal length of the proposed BPLC lens: black solid curve is for wave 1 and red dashed curve is for wave 2.

4. Conclusion

We proposed a new polymer-stabilized blue-phase lens using a resistive electrode. At low fields, when the induced birefringence follows the Kerr effect, a parabolic phase profile is formed without any pixelated electrodes. For an optimized structure with cell gap 13 μm and aperture radius100 μm, as the applied voltage V_o is varied from 0 to $50V_{\mathrm{rms}}$, focal length could be continuously tuned from ∞ to 18 mm. Through the whole focal length range, the lens could maintain polarization independent and parabolic shape. Such a device, with only a single cell gap, planar electrodes, and single data addressing, is easy to fabricate and would be very attractive for a wide range of applications that need miniaturized autofocus.

The authors are indebted to Jin Yan and Su Xu for useful discussion and financial support from Industrial Technology Research Institute (Taiwan).

References

1. S. Sato, "Liquid-crystal lens-cells with variable focal length," Jpn. J. Appl. Phys. **18**, 1679–1684 (1979).
2. S. T. Kowel, D. S. Cleverly, and P. G. Kornreich, "Focusing by electrical modulation of refraction in a liquid crystal cell," Appl. Opt. **23**, 278–289 (1984).
3. N. A. Riza and M. C. DeJule, "Three-terminal adaptive nematic liquid crystal lens device," Opt. Lett. **19**, 1013–1015 (1994).
4. H. Ren, Y. H. Fan, and S. T. Wu, "Tunable Fresnel lens using nanoscale polymer-dispersed liquid crystals," Appl. Phys. Lett. **83**, 1515–1517 (2003).
5. H. Ren, Y. H. Fan, S. Gauza, and S. T. Wu, "Tunable-focus flat liquid crystal spherical lens," Appl. Phys. Lett. **84**, 4789–4791 (2004).
6. Y. H. Fan, H. Ren, X. Liang, H. Wang, and S. T. Wu, "Liquid crystal microlens arrays with switchable positive and negative focal lengths," J. Display Technol. **1**, 151–156 (2005).
7. H. Ren, D. Fox, B. Wu, and S. T. Wu, "Liquid crystal lens with large focal length tunability and low operating voltage," Opt. Express **15**, 11328–11335 (2007).
8. M. Ye and S. Sato, "Optical properties of liquid crystal lens of any size," Jpn. J. Appl. Phys. **41**, L571–L573 (2002).
9. H. Ren, Y. H. Fan, S. Gauza, and S. T. Wu, "Tunable-focus cylindrical liquid crystal lens," Jpn. J. Appl. Phys. **43**, 652–653 (2004).
10. B. Wang, M. Ye, and S. Sato, "Liquid crystal lens with focal length variable from negative to positive values," IEEE Photon. Technol. Lett. **18**, 79–81 (2006).
11. Y. P. Huang, C. W. Chen, and T. C. Shen, "High resolution autostereoscopic 3D display with scanning multielectrode driving

liquid crystal (MeD-LC) lens," Soc. Inf. Display Tech. Digest **40**, 336–339 (2009).
12. Y. Y. Kao, P. C. P. Chao, and C. W. Hsueh, "A new low-voltage-driven GRIN liquid crystal lens with multiple ring electrodes in unequal widths," Opt. Express **18**, 18506–18518 (2010).
13. A. F. Naumov, G. D. Love, M. Yu. Loktev, and F. L. Vladimirov, "Control optimization of spherical modal liquid crystal lenses," Opt. Express **4**, 344–352 (1999).
14. N. Fraval and J. L. B. de la Tocnaye, "Low aberrations symmetrical adaptive modal liquid crystal lens with short focal lengths," Appl. Opt. **49**, 2778–2783 (2010).
15. H. Kikuchi, M. Yokota, Y. Hiskado, H. Yang, and T. Kajiyama, "Polymer-stabilized liquid crystal blue phases," Nat. Mater. **1**, 64–68 (2002).
16. Y. Haseba, H. Kikuchi, T. Nagamura, and T. Kajiyama, "Large electro-optic Kerr effect in nanostructured chiral liquid-crystal composites over a wide temperature range," Adv. Mater. **17**, 2311 (2005).
17. Z. Ge, S. Gauza, M. Jiao, H. Xianyu, and S. T. Wu, "Electro-optics of polymer-stabilized blue phase liquid crystal displays," Appl. Phys. Lett. **94**, 101104 (2009).
18. Z. Ge, L. Rao, S. Gauza, and S. T. Wu, "Modeling of blue phase liquid crystal displays," J. Display Technol. **5**, 250–256 (2009).
19. L. Rao, Z. Ge, S. T. Wu, and S. H. Lee, "Low voltage blue-phase liquid crystal displays," Appl. Phys. Lett. **95**, 231101 (2009).
20. Y. Li, Y. Chen, J. Sun, S. T. Wu, S. H. Liu, P. J. Hsieh, K. L. Cheng, and J. W. Shiu, "Dielectric dispersion on the Kerr constant of blue phase liquid crystals," Appl. Phys. Lett. **99**, 181126 (2011).
21. J. Yan, Y. Li, and S. T. Wu, "High-efficiency and fast-response tunable phase grating using a blue phase liquid crystal," Opt. Lett. **36**, 1404–1406 (2011).
22. K. M. Chen, S. Gauza, H. Xianyu, and S. T. Wu, "Submillisecond gray-level response time of a polymer-stabilized blue-phase liquid crystal," J. Display Technol. **6**, 49–51 (2010).
23. Y. Chen, J. Yan, J. Sun, S. T. Wu, X. Liang, S. H. Liu, P. J. Hsieh, K. L. Cheng, and J. W. Shiu, "A microsecond-response polymer-stabilized blue-phase liquid crystal," Appl. Phys. Lett. **99**, 201105 (2011).
24. Y. H. Lin, H. S. Chen, H. C. Lin, Y. S. Tsou, H. K. Hsu, and W. Y. Li, "Polarizer-free and fast response microlens arrays using polymer-stabilized blue phase liquid crystals," Appl. Phys. Lett. **96**, 113505 (2010).
25. Y. Li and S. T. Wu, "Polarization independent adaptive microlens with a blue-phase liquid crystal," Opt. Express **19**, 8045–8050 (2011).
26. C. T. Lee, Y. Li, H. Y. Lin, and S. T. Wu, "Design of polarization-independent multi-electrode GRIN lens with a blue-phase liquid crystal," Opt. Express **19**, 17402–17407 (2011).
27. A. F. Naumov and G. Vdovin, "Multichannel liquid-crystal-based wave-front corrector with modal influence functions," Opt. Lett. **23**, 1550–1552 (1998).
28. A. F. Naumov, M. Yu. Loktev, I. R. Guralnik, and G. Vdovin, "Liquid-crystal adaptive lenses with modal control," Opt. Lett. **23**, 992–994 (1998).
29. J. Kerr, "A new relation between electricity and light: dielectrified media birefringent," Philos. Mag. **50**, 337–348 (1875).
30. J. Yan, H. C. Cheng, S. Gauza, Y. Li, M. Jiao, L. Rao, and S. T. Wu, "Extended Kerr effect of polymer-stabilized blue-phase liquid crystals," Appl. Phys. Lett. **96**, 071105 (2010).
31. H. C. Cheng, J. Yan, T. Ishinabe, and S. T. Wu, "Vertical field switching for blue-phase liquid crystal devices," Appl. Phys. Lett. **98**, 261102 (2011).
32. M. Jiao, J. Yan, and S. T. Wu, "Dispersion relation on the Kerr constant of a polymer-stabilized optically isotropic liquid crystal," Phys. Rev. E **83**, 041706 (2011).